Eleventh International Conference on Computational Fluid Dynamics (ICCFD11), Maui, HI, July 11-15, 2022

ICCFD11-2022-0401

Stable and non-dissipative kinetic-energy and entropy preserving (KEEP) schemes for compressible flows

Y. Kuya* and S. Kawai*
Corresponding author: kuya@tohoku.ac.jp

* Department of Aerospace Engineering, Tohoku University, Sendai, Miyagi, 980-8579, Japan.

Abstract: Stable and non-dissipative kinetic-energy and entropy preserving (KEEP) schemes have been proposed for compressible flows. The KEEP schemes significantly improve numerical robustness compared to the kinetic energy preserving (KEP) schemes, which are widely recognized as non-dissipative and stable numerical schemes. Our research group has recently succeeded in conducting wall-modeled large-eddy simulations of whole aircraft configurations using the KEEP schemes, where no numerical dissipation is employed for numerical stabilization. The present study comprehensively discusses the recent progress in our research related to the KEEP schemes, including the derivation background and numerical formulations.

Keywords: Non-dissipative numerical schemes, Kinetic energy and entropy preservation, Split convective forms, Compressible flows.

1 Introduction

There have been high expectations for a high-fidelity flow analysis of high Reynolds number compressible flows around complex geometries using large eddy simulation (LES) for a long time. In order to conduct high-fidelity flow computations, it is widely recognized that employing non-dissipative and stable numerical schemes is crucial. Among the existing non-dissipative and stable numerical schemes, kinetic energy preserving (KEP) schemes [1, 2, 3, 4, 5] are well known. The KEP schemes are based on central difference approximations, i.e., non-dissipative, but numerically stable thanks to their kinetic energy preservation property. The authors have significantly improved the numerical stability of the KEP schemes, particularly for the flows in which the compressibility effects appear, by enhancing the entropy preservation property of the KEP schemes; accordingly, hereafter, we refer to the those numerical schemes as kinetic energy and entropy preserving (KEEP) schemes. The authors, together with our research group members, have shown progress on the following research subjects related to the KEEP schemes:

1. Second-order accurate KEEP scheme in Cartesian coordinates [6]
2. Kinetic energy and entropy preservation at non-conforming block boundaries on block-structured Cartesian grids [7]
3. High-order accurate KEEP scheme on generalized curvilinear grids [8]
4. Split convective form maintaining velocity and pressure equilibrium at contact discontinuity [9]
5. Entropy conservation error analysis of KEEP schemes [10]
6. Spectral characteristics of split convective forms in finite difference methods [11]
7. A spatially and temporally conservative KEEP scheme [12]
8. A KEEP scheme for unstructured finite volume methods [13]

The primary objective of the KEEP scheme development is to construct non-dissipative and stable numerical schemes for realizing high Reynolds number LES around complex geometries. In addition to employing stable and non-dissipative numerical schemes, two more requirements may need to be satisfied in order to realize high Reynolds number LES around complex geometries: 1) numerical schemes are applicable to complex geometries, and 2) near-wall turbulence is solved accurately and efficiently. Although upwind schemes are generally used to conduct flow computations around complex geometries, those numerical schemes are not suitable for high-fidelity computations due to their numerical dissipation. To meet the first requirement using non-dissipative schemes (i.e., KEEP schemes), our research group has developed a block-structured Cartesian solver called FFVHC-ACE, where the second-order accurate KEEP scheme [6] is implemented. In the block block-structured Cartesian solver, non-conforming block boundaries (or hanging nodes) appear when the grid resolution is different across the block boundaries. To deal with such non-conforming boundaries, we proposed a non-dissipative and stable approach that leads to kinetic energy and entropy preservation at the non-conforming boundaries [7]. Moreover, in order to meet the second requirement mentioned above, our research group developed an LES wall model that can deal with non-grid-conforming wall boundaries [14] and is also implemented in FFVHC-ACE.

Those KEEP schemes [6, 7] and the wall model [14] have proven to be beneficial in performing high Reynolds number LES around complex geometries stably and non-dissipatively; for example, Asada and Kawai [15] and Tamaki et al. [16], where high-Reynolds number LES of whole aircraft configurations were performed. In those studies, since the KEEP schemes do not require numerical dissipation for numerical stabilization, the LES obtained by the KEEP schemes exhibit remarkably better accuracy on a smaller number of computational grids compared to those obtained by an upwind scheme.

The present study comprehensively discusses the KEEP schemes and related subjects, focusing in particular on the first to third research subjects listed above. The rest of this paper is organized as follows. Section 2 describes the KEEP schemes proposed in Refs. [6, 7, 11], corresponding to the first to third research subjects listed above. The other research subjects are briefly discussed in Section 3. In Section 4, numerical tests are conducted using the KEEP schemes. Concluding remarks are given in Section 5.

2 KEEP schemes

2.1 Derivation background

The governing equations we consider here are the compressible Euler equations:

$$\frac{\partial Q}{\partial t}+\frac{\partial F_j}{\partial x_j}=0,\ Q=\begin{bmatrix}\rho\\ \rho u_i\\ E\end{bmatrix},\ F_j=\begin{bmatrix}\rho u_j\\ \rho u_i u_j+p\delta_{ij}\\ (E+p)u_j\end{bmatrix}, \tag{1}$$

where ρ is the density, u_i is the velocity component in the i-direction, and p is the pressure. The total energy E is the sum of the kinetic energy and internal energy: $E{=}\rho k{+}\rho e$, where $k{=}u_i u_i/2$. The total energy equation in Eq. (1) can be decomposed into the kinetic energy equation

$$\frac{\partial \rho k}{\partial t}+\frac{\partial \rho k u_j}{\partial x_j}+u_j\frac{\partial p}{\partial x_j}=0, \tag{2}$$

and the internal energy equation

$$\frac{\partial \rho e}{\partial t}+\frac{\partial \rho e u_j}{\partial x_j}+p\frac{\partial u_j}{\partial x_j}=0. \tag{3}$$

Eq. (2) indicates that the total kinetic energy is only preserved in the incompressible and inviscid limits. Under the assumption of an ideal gas, the internal energy can be written as $e{=}p/(\rho(\gamma-1))$, where γ is the ratio of specific heats.

The kinetic energy equation in Eq. (2) can be derived from the mass and momentum equations as:

$$[-k,u_i]\left\{\frac{\partial}{\partial t}\begin{bmatrix}\rho\\ \rho u_i\end{bmatrix}+\frac{\partial}{\partial x_j}\begin{bmatrix}\rho u_j\\ \rho u_i u_j+p\delta_{ij}\end{bmatrix}\right\}=0\ \Rightarrow\ \frac{\partial \rho k}{\partial t}+\frac{\partial \rho k u_j}{\partial x_j}+u_j\frac{\partial p}{\partial x_j}=0. \tag{4}$$

On the other hand, as shown in Ref. [3], the entropy equation may be derived from the Gibbs equation as

$$\frac{\partial \rho s}{\partial t} + \frac{\partial \rho s u_j}{\partial x_j} = \frac{1}{T}\left[\left(sT - e - \frac{p}{\rho}\right)\left(\underbrace{\frac{\partial \rho}{\partial t} + \frac{\partial \rho u_j}{\partial x_j}}_{\text{Mass equation}}\right) + \underbrace{\frac{\partial \rho e}{\partial t} + \frac{\partial \rho e u_j}{\partial x_j} + p\frac{\partial u_j}{\partial x_j}}_{\text{Internal energy equation}}\right], \tag{5}$$

where s=log$(p\rho^{-\gamma})$ is the entropy, and T is the temperature. The mass equation appearing on the right-hand side of Eq. (5) is directly discretized and solved in compressible flow computations, and thus $\frac{\partial \rho}{\partial t} + \frac{\partial \rho u_j}{\partial x_j} = 0$ is satisfied. For entropy conservation, the internal energy equation appearing on the right-hand side of Eq. (5) also needs to satisfy $\frac{\partial \rho e}{\partial t} + \frac{\partial \rho e u_j}{\partial x_j} + p\frac{\partial u_j}{\partial x_j} = 0$. However, in general, the internal energy equation is not solved directly in compressible flow computations but is solved as part of the total energy equation to be a conservative formulation. Accordingly, it is important to accurately solve the balance of the kinetic energy and internal energy equations in the total energy equation for kinetic energy and entropy preservation. To achieve the correct computations of the energy exchange in the total energy equation, we impose constraints such that the KEEP schemes numerically duplicate the following three analytical relations that the governing equations hold:

1. The kinetic energy equation is derived from the mass and momentum equations: Eq. (4).

2. The kinetic energy and internal energy are convected by the same convective velocity u_j:

$$\frac{\partial \rho k u_j}{\partial x_j} + \frac{\partial \rho e u_j}{\partial x_j} = \frac{\partial \rho (k+e) u_j}{\partial x_j}. \tag{6}$$

3. The pressure-diffusion term in the total energy equation is the sum of the pressure-work term in the kinetic energy equation and the pressure-dilatation term in the internal energy equation:

$$\frac{\partial u_j p}{\partial x_j} = u_j \frac{\partial p}{\partial x_j} + p\frac{\partial u_j}{\partial x_j}. \tag{7}$$

One thing to note here is that although the KEEP schemes improve the entropy preservation property of the existing KEP schemes, leading to much better numerical robustness, the KEEP schemes do not guarantee that the entropy convection term in Eq. (5) is calculated conservatively, so the entropy is not conserved to machine precision in the KEEP schemes; a detailed analysis of the entropy conservation property of the KEEP schemes is shown in Tamaki et al. [10]. Nevertheless, the KEEP schemes have shown superior numerical stability in both typical academic test cases [6, 7, 8] and practical applications [15, 16].

2.2 Second-order accurate KEEP scheme in Cartesian coordinates

The second-order accurate KEEP schemes in Cartesian coordinates proposed in Ref. [6] are described here. The derivatives in Eq. (1) are discretized using the numerical fluxes as

$$\begin{aligned}
&\frac{\partial \rho u_j}{\partial x_j} \simeq \frac{\widetilde{\mathcal{C}}_j|_{(m+\frac{1}{2})} - \widetilde{\mathcal{C}}_j|_{(m-\frac{1}{2})}}{\Delta x_j}, \quad \frac{\partial \rho u_i u_j}{\partial x_j} \simeq \frac{\widetilde{\mathcal{M}}_{ij}|_{(m+\frac{1}{2})} - \widetilde{\mathcal{M}}_{ij}|_{(m-\frac{1}{2})}}{\Delta x_j}, \quad \frac{\partial \rho k u_j}{\partial x_j} \simeq \frac{\widetilde{\mathcal{K}}_j|_{(m+\frac{1}{2})} - \widetilde{\mathcal{K}}_j|_{(m-\frac{1}{2})}}{\Delta x_j}, \\
&\frac{\partial \rho e u_j}{\partial x_j} \simeq \frac{\widetilde{\mathcal{I}}_j|_{(m+\frac{1}{2})} - \widetilde{\mathcal{I}}_j|_{(m-\frac{1}{2})}}{\Delta x_j}, \quad \frac{\partial p\delta_{ij}}{\partial x_j} \simeq \frac{\widetilde{\mathcal{G}}_{ij}|_{(m+\frac{1}{2})} - \widetilde{\mathcal{G}}_{ij}|_{(m-\frac{1}{2})}}{\Delta x_j}, \quad \frac{\partial u_j p}{\partial x_j} \simeq \frac{\widetilde{\mathcal{P}}_j|_{(m+\frac{1}{2})} - \widetilde{\mathcal{P}}_j|_{(m-\frac{1}{2})}}{\Delta x_j}.
\end{aligned} \tag{8}$$

$\widetilde{\mathcal{C}}$, $\widetilde{\mathcal{M}}$, $\widetilde{\mathcal{K}}$, $\widetilde{\mathcal{I}}$, $\widetilde{\mathcal{G}}$, and $\widetilde{\mathcal{P}}$ are the numerical fluxes of the mass, momentum, kinetic energy, and internal energy, pressure-gradient, and pressure-diffusion terms, respectively. m denotes the node index, and the numerical fluxes are defined at the half-point faces $m \pm \frac{1}{2}$. The second-order accurate KEEP numerical fluxes proposed in Ref. [6] are:

$$
\begin{aligned}
\widetilde{\mathcal{C}}_j|_{(m\pm\frac{1}{2})} &\equiv \frac{\rho|_{(m)}+\rho|_{(m\pm1)}}{2}\frac{u_j|_{(m)}+u_j|_{(m\pm1)}}{2},\\
\widetilde{\mathcal{M}}_{ij}|_{(m\pm\frac{1}{2})} &\equiv \frac{\rho|_{(m)}+\rho|_{(m\pm1)}}{2}\frac{u_i|_{(m)}+u_i|_{(m\pm1)}}{2}\frac{u_j|_{(m)}+u_j|_{(m\pm1)}}{2} = \widetilde{\mathcal{C}}_j|_{(m\pm\frac{1}{2})}\frac{u_i|_{(m)}+u_i|_{(m\pm1)}}{2},\\
\widetilde{\mathcal{K}}_j|_{(m\pm\frac{1}{2})} &\equiv \frac{\rho|_{(m)}+\rho|_{(m\pm1)}}{2}\frac{u_i|_{(m)}u_i|_{(m\pm1)}}{2}\frac{u_j|_{(m)}+u_j|_{(m\pm1)}}{2} = \widetilde{\mathcal{C}}_j|_{(m\pm\frac{1}{2})}\frac{u_i|_{(m)}u_i|_{(m\pm1)}}{2},\\
\widetilde{\mathcal{I}}_j|_{(m\pm\frac{1}{2})} &\equiv \frac{\rho|_{(m)}+\rho|_{(m\pm1)}}{2}\frac{e|_{(m)}+e|_{(m\pm1)}}{2}\frac{u_j|_{(m)}+u_j|_{(m\pm1)}}{2} = \widetilde{\mathcal{C}}_j|_{(m\pm\frac{1}{2})}\frac{e|_{(m)}+e|_{(m\pm1)}}{2},\\
&\left(= \widetilde{\mathcal{C}}_j|_{(m\pm\frac{1}{2})}\frac{(p/\rho)|_{(m)}+(p/\rho)|_{(m\pm1)}}{2(\gamma-1)}\right)\\
\widetilde{\mathcal{G}}_{ij}|_{(m\pm\frac{1}{2})} &\equiv \frac{(p\delta_{ij})|_{(m)}+(p\delta_{ij})|_{(m\pm1)}}{2},\\
\widetilde{\mathcal{P}}_j|_{(m\pm\frac{1}{2})} &\equiv \frac{u_j|_{(m)}p|_{(m\pm1)}+u_j|_{(m\pm1)}p|_{(m)}}{2}.
\end{aligned}
\tag{9}
$$

These KEEP numerical fluxes numerically hold the aforementioned analytical relations. The kinetic energy numerical flux is derived by substituting the mass and momentum numerical fluxes into the first analytical relation of Eq. (4):

$$
\widetilde{\mathcal{K}}_j = -k|_{(m)}\widetilde{\mathcal{C}}_j + u_i|_{(m)}\widetilde{\mathcal{M}}_{ij}. \tag{10}
$$

The internal energy numerical flux is derived following the second analytical relation of Eq. (6):

$$
\widetilde{\mathcal{K}}_j + \widetilde{\mathcal{I}}_j = \frac{\rho|_{(m)}+\rho|_{(m\pm1)}}{2}\left(\underbrace{\frac{u_i|_{(m)}u_i|_{(m\pm1)}}{2}}_{\text{Kinetic energy}} + \underbrace{\frac{e|_{(m)}+e|_{(m\pm1)}}{2}}_{\text{Internal energy}}\right)\frac{u_j|_{(m)}+u_j|_{(m\pm1)}}{2}. \tag{11}
$$

The pressure-diffusion numerical flux discretely satisfies the product rule in Eq. (7) (i.e., third analytical relation) as

$$
\begin{aligned}
\frac{\partial u_j p}{\partial x_j} &\simeq \frac{\dfrac{u_j|_{(m)}p|_{(m+1)}+u_j|_{(m+1)}p|_{(m)}}{2} - \dfrac{u_j|_{(m)}p|_{(m-1)}+u_j|_{(m-1)}p|_{(m)}}{2}}{\Delta x_j},\\
&= u_j|_{(m)}\frac{p|_{(m+1)}-p|_{(m-1)}}{2\Delta x_j} + p|_{(m)}\frac{u_j|_{(m+1)}-u_j|_{(m-1)}}{2\Delta x_j}.
\end{aligned}
\tag{12}
$$

In Ref. [6], it is exhibited that the entropy preservation property is impaired if any of the analytical relations is not discretely retained. Further details of the second-order accurate KEEP scheme in Cartesian coordinates are discussed in Ref. [6].

2.3 Kinetic energy and entropy preservation at hanging node boundaries on Cartesian grids

When Asada and Kawai [15] and Tamaki et al. [16] realized high-Reynolds number LES of whole aircraft configurations using the LES wall model [14] and the KEEP schemes [6, 7], a block-structured Cartesian solver called FFVHC-ACE was used. As is well known, one of the strong advantages of block-structured Cartesian solvers is that the resolution of computational grids can be efficiently controlled. On the other hand, one drawback of block-structured Cartesian solvers may be the need to deal with non-conforming block boundaries (i.e., handing nodes), where the grid resolution is different across the computational block boundaries. Not all block-structured Cartesian solvers satisfy even the conservation of the primary conservative quantities, i.e., mass, momentum, and total energy, at non-conforming block boundaries.

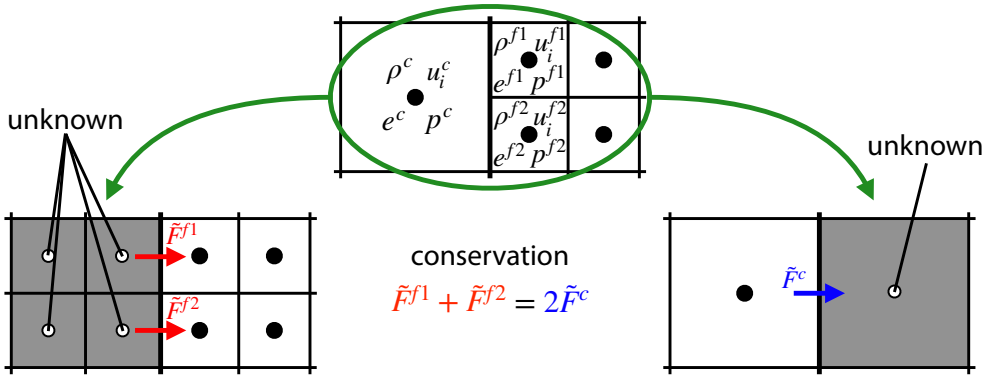

Figure 1: Treatment of non-conforming block boundaries using ghost cells in two dimensions. Ghost cells are colored by gray. Appropriate values are given to the ghost cells so that all the KEEP numerical fluxes satisfy conservation, leading to kinetic energy and entropy preservation, as well as the conservation of the primary conservative quantities.

In Ref. [7], we proposed a numerical method that maintains kinetic energy and entropy preservation at non-conforming block boundaries and the conservation of the mass, momentum, and total energy. A schematic of the proposed approach is shown in Fig. 1. In the proposed approach, ghost cells are introduced, and appropriate values are given to the ghost cells so that all the KEEP numerical fluxes shown in Eq. (9) satisfy kinetic energy and entropy preservation at non-conforming block boundaries, as well as the conservation of the primary conservative quantities. For conservation, the following relation should be satisfied at non-conforming block boundaries in two dimensions:

$$\tilde{F}^{f1} + \tilde{F}^{f2} = 2\tilde{F}^{c}, \tag{13}$$

where $\tilde{F}^{f1}$ and $\tilde{F}^{f2}$ are the numerical fluxes between the fine ghost cells and fine fluid cells, while $\tilde{F}^{c}$ is the numerical flux between the coarse ghost cell and coarse fluid cell. The fine and coarse fluid cells contain the following primitive quantities:

- Fine cell $(f1)$: ρ^{f1}, u_i^{f1}, e^{f1}, p^{f1}
- Fine cell $(f2)$: ρ^{f2}, u_i^{f2}, e^{f2}, p^{f2}
- Coarse cell (c): ρ^{c}, u_i^{c}, e^{c}, p^{c}

The pressure p may be obtained from the density ρ and the internal energy e using the ideal gas law. We employ the piecewise constant approximation for the fine ghost cells, i.e., simply copy the values in the coarse fluid cell to the fine ghost cells. Given the fine ghost cell values, the fine cell fluxes of $\tilde{F}^{f1}$ and $\tilde{F}^{f2}$ can be calculated, and thus the left-hand side of Eq. (13) can be obtained. Consequently, we obtain the coarse ghost cell values such that all the KEEP numerical fluxes in Eq. (9) satisfy Eq. (13) as

$$\begin{aligned}
\hat{\rho} &= \frac{1}{2}\frac{\rho^{f1}(u^{f1}+u^{c}) + \rho^{f2}(u^{f2}+u^{c}) + \rho^{c}(u^{f1}+u^{f2}-2\hat{u})}{u^{c}+\hat{u}+\epsilon}, \\
\hat{u} &= \frac{(\rho^{f1}+\rho^{c})(u^{f1}+u^{c})u^{f1} + (\rho^{f2}+\rho^{c})(u^{f2}+u^{c})u^{f2}}{\rho^{f1}(u^{f1}+u^{c}) + \rho^{f2}(u^{f2}+u^{c}) + \rho^{c}(u^{f1}+u^{f2}+2u^{c}) + \epsilon}, \\
\hat{e} &= \frac{(\rho^{f1}+\rho^{c})(u^{f1}+u^{c})e^{f1} + (\rho^{f2}+\rho^{c})(u^{f2}+u^{c})e^{f2}}{\rho^{f1}(u^{f1}+u^{c}) + \rho^{f2}(u^{f2}+u^{c}) + \rho_{c}(u^{f1}+u^{f2}+2u^{c}) + \epsilon},
\end{aligned} \tag{14}$$

and

$$\begin{aligned} \hat{u}_p &= \frac{u^{f1} + u^{f2}}{2}, \\ \hat{p}_p &= \frac{p^{f1} + p^{f2}}{2}, \end{aligned} \tag{15}$$

where *hat* denotes the coarse ghost cell values, and ϵ is a minimal positive value that prevents the computational divergence due to the denominator of Eq. (14) becoming zero. Eq. (14) is used for the computations of the convective terms, while Eq. (15) is used for the computations of the pressure-related terms (i.e., pressure-gradient and pressure-diffusion terms). By giving the values to the fine ghost cells with the piecewise constant approximation and the coarse ghost cell with Eqs. (14) and (15), kinetic energy and entropy preservation is satisfied even at such non-conforming block boundaries, leading to non-dissipative and stable flow computations of complex geometries. More detailed derivations are described in Ref. [7].

2.4 High-order accurate KEEP scheme in generalized curvilinear coordinates

This subsection describes high-order accurate KEEP scheme in generalized curvilinear coordinates. The above two subsections discuss the second-order accurate KEEP schemes for block-structured Cartesian solvers. Although the combination of those second-order accurate KEEP schemes and a block-structured Cartesian solver has proven useful in performing high-fidelity flow computations of compressible flows around complex geometries, it is also beneficial to extend the KEEP schemes to curvilinear coordinate systems. Furthermore, for example, in aeroacoustic problems, it is important to reduce dispersion errors in addition to dissipation errors, and thus the extension of the KEEP scheme to higher-order accuracy is also beneficial for performing high-fidelity flow computations.

The Euler equations in generalized curvilinear coordinates (ξ_1, ξ_2, ξ_3) are

$$\frac{\partial \hat{Q}}{\partial t} + \frac{\partial \hat{F}_j}{\partial \xi_j} = 0,\ \hat{Q} = \frac{1}{J}\begin{bmatrix} \rho \\ \rho u_i \\ E \end{bmatrix},\ \hat{F}_j = \frac{1}{J}\begin{bmatrix} \rho U_j \\ \rho u_i U_j + \xi^x_{ji} p \\ (E+p)U_j \end{bmatrix}, \tag{16}$$

where $\xi^x_{ji}(=\partial \xi_j / \partial x_i)$ and J are the grid metrics and Jacobian defined for the coordinate transformation, and $U_j(=\xi^x_{j\ell} u_\ell)$ is the contravariant velocity component. When the KEEP schemes in generalized curvilinear coordinates are developed, we utilizes the relation that the ξ_j-direction flux $\hat{F}_j$ can be obtained by the inner product between the inviscid flux vector F_ℓ and the surface-normal area vector $\xi^x_{j\ell}/J$ as

$$\hat{F}_j = (\xi^x_{j\ell}/J) F_\ell. \tag{17}$$

As same as the KEEP schemes in Cartesian coordinates shown in Eqs. (8) and (9), we discretize the spacial derivatives in Eq. (16) using numerical fluxes as

$$\begin{aligned} &\frac{\partial \rho U_j/J}{\partial \xi_j} \simeq \frac{\widehat{\mathcal{C}}_j|_{(m+\frac{1}{2})} - \widehat{\mathcal{C}}_j|_{(m-\frac{1}{2})}}{\Delta \xi_j},\ \frac{\partial \rho u_i U_j/J}{\partial \xi_j} \simeq \frac{\widehat{\mathcal{M}}_{ij}|_{(m+\frac{1}{2})} - \widehat{\mathcal{M}}_{ij}|_{(m-\frac{1}{2})}}{\Delta \xi_j},\ \frac{\partial \rho k U_j/J}{\partial \xi_j} \simeq \frac{\widehat{\mathcal{K}}_j|_{(m+\frac{1}{2})} - \widehat{\mathcal{K}}_j|_{(m-\frac{1}{2})}}{\Delta \xi_j}, \\ &\frac{\partial \rho e U_j/J}{\partial \xi_j} \simeq \frac{\widehat{\mathcal{I}}_j|_{(m+\frac{1}{2})} - \widehat{\mathcal{I}}_j|_{(m-\frac{1}{2})}}{\Delta \xi_j},\ \frac{\partial (\xi^x_{ji}/J) p}{\partial \xi_j} \simeq \frac{\widehat{\mathcal{G}}_{ij}|_{(m+\frac{1}{2})} - \widehat{\mathcal{G}}_{ij}|_{(m-\frac{1}{2})}}{\Delta \xi_j},\ \frac{\partial U_j p/J}{\partial \xi_j} \simeq \frac{\widehat{\mathcal{P}}_j|_{(m+\frac{1}{2})} - \widehat{\mathcal{P}}_j|_{(m-\frac{1}{2})}}{\Delta \xi_j}, \end{aligned} \tag{18}$$

where $\widehat{\mathcal{C}}$, $\widehat{\mathcal{M}}$, $\widehat{\mathcal{K}}$, $\widehat{\mathcal{I}}$, $\widehat{\mathcal{G}}$, and $\widehat{\mathcal{P}}$ are the numerical fluxes of the mass, momentum, kinetic energy, internal energy, pressure-gradient, and pressure-diffusion terms in generalized curvilinear coordinates, respectively. The numerical fluxes of the high-order accurate KEEP schemes in generalized curvilinear coordinates proposed in Ref. [8] are:

$$
\begin{aligned}
\widehat{\mathcal{C}}_j|_{(m\pm\frac{1}{2})} &\equiv 2\sum_{m_s=1}^{q/2} a_{q,m_s} \sum_{n=0}^{m_s-1} \frac{\rho|_{(m\mp n)}+\rho|_{(m\mp n\pm m_s)}}{2} \frac{(\xi^x_{j\ell}/J)|_{(m\mp n)}+(\xi^x_{j\ell}/J)|_{(m\mp n\pm m_s)}}{2} \frac{u_\ell|_{(m\mp n)}+u_\ell|_{(m\mp n\pm m_s)}}{2} \\
&= 2\sum_{m_s=1}^{q/2} a_{q,m_s} \sum_{n=0}^{m_s-1} \widehat{\mathcal{C}}^*_j|_{(m\pm\frac{1}{2})}, \\
\widehat{\mathcal{M}}_{ij}|_{(m\pm\frac{1}{2})} &\equiv 2\sum_{m_s=1}^{q/2} a_{q,m_s} \sum_{n=0}^{m_s-1} \widehat{\mathcal{C}}^*_j|_{(m\pm\frac{1}{2})} \frac{u_i|_{(m\mp n)}+u_i|_{(m\mp n\pm m_s)}}{2}, \\
\widehat{\mathcal{K}}_j|_{(m\pm\frac{1}{2})} &\equiv 2\sum_{m_s=1}^{q/2} a_{q,m_s} \sum_{n=0}^{m_s-1} \widehat{\mathcal{C}}^*_j|_{(m\pm\frac{1}{2})} \frac{u_i|_{(m\mp n)}u_i|_{(m\mp n\pm m_s)}}{2}, \\
\widehat{\mathcal{I}}_j|_{(m\pm\frac{1}{2})} &\equiv 2\sum_{m_s=1}^{q/2} a_{q,m_s} \sum_{n=0}^{m_s-1} \widehat{\mathcal{C}}^*_j|_{(m\pm\frac{1}{2})} \frac{e|_{(m\mp n)}+e|_{(m\mp n\pm m_s)}}{2}, \\
&\left(= 2\sum_{m_s=1}^{q/2} a_{q,m_s} \sum_{n=0}^{m_s-1} \widehat{\mathcal{C}}^*_j|_{(m\pm\frac{1}{2})} \frac{(p/\rho)|_{(m\mp n)}+(p/\rho)|_{(m\mp n\pm m_s)}}{2(\gamma-1)}, \right) \\
\widehat{\mathcal{G}}_{ij}|_{(m\pm\frac{1}{2})} &\equiv 2\sum_{m_s=1}^{q/2} a_{q,m_s} \sum_{n=0}^{m_s-1} \frac{(\xi^x_{ji}/J)|_{(m\mp n)}+(\xi^x_{ji}/J)|_{(m\mp n\pm m_s)}}{2} \frac{p|_{(m\mp n)}+p|_{(m\mp n\pm m_s)}}{2}, \\
\widehat{\mathcal{P}}_j|_{(m+\frac{1}{2})} &\equiv 2\sum_{m_s=1}^{q/2} a_{q,m_s} \sum_{n=0}^{m_s-1} \frac{u_i|_{(m)}p|_{(m+1)}+u_i|_{(m+1)}p|_{(m)}}{2} \frac{(\xi^x_{ji}/J)|_{(m)}+(\xi^x_{ji}/J)|_{(m+1)}}{2}.
\end{aligned}
\tag{19}
$$

Here, the high-order extension is achieved by following the approach proposed by Pirozzoli [4]. Ref. [8] also constructed a high-order accurate KEEP scheme in generalized curvilinear coordinates by using compact difference approximations. Ignoring the summation in Eq. (19), it can be recognized that the KEEP numerical fluxes in generalized curvilinear coordinates in Eq. (19) satisfy the relation of Eq. (17) with the KEEP numerical fluxes in Cartesian coordinates in Eq. (9). The important aspect in the derivation of the curvilinear coordinate formulations is that the area vector component (ξ^x_{ji}/J) is defined at the half-point faces, regarding the area vector component as another individual variable in addition to the physical variables, such as the density, velocity, and pressure. More details about the high-order accurate KEEP schemes in generalized curvilinear coordinates are described in Ref. [8].

3 Other research subjects related to KEEP schemes

In the previous section, we summarizes our recent achievements related to the first to third research subjects given in Section 1. In this section, the other research subjects, i.e., the fourth to eighth research subjects, are also briefly discussed.

3.1 Split convective form maintaining velocity and pressure equilibrium at contact discontinuity

Shima et al. [9] showed that the split convective forms used in the KEEP schemes [6] and typical KEP schemes [1, 4, 5] induce spurious oscillations at contact discontinuity. Also, they proposed a new internal energy numerical flux that maintains the velocity and pressure equilibrium at contact discontinuity holding the good kinetic energy and entropy preservation property of the KEEP schemes:

$$
\widetilde{\mathcal{I}}_j|_{(m\pm\frac{1}{2})} \equiv \frac{(\rho e)|_{(m)}+(\rho+e)|_{(m\pm1)}}{2} \frac{u_j|_{(m)}+u_j|_{(m\pm1)}}{2} \left(= \frac{p|_{(m)}+p|_{(m\pm1)}}{2(\gamma-1)} \frac{u_j|_{(m)}+u_j|_{(m\pm1)}}{2} \right). \tag{20}
$$

The modified internal-energy numerical flux proposed in Shima et al. [9] was of second-order accuracy in space on Cartesian grids. However, extending Eq. (20) to a high-order formulation on curvilinear grids is straightforward, according to the approach proposed in section 2.4 and Refs. [4, 8].

3.2 Entropy conservation error analysis of KEEP schemes

As described in section 2.1, the KEEP schemes are derived such that the numerical fluxes discretely satisfy the three analytical relations that the governing equations hold. Also, the numerical tests performed in Ref. [6] showed that if any of the analytical relations are broken, the entropy conservation property is severely compromised, and the computations become unstable. Tamaki et al. [10] derived a discrete entropy conservation equation and analyzed the entropy conservation property of the KEEP scheme. The superior numerical robustness of the KEEP schemes has been confirmed by numerical tests. However, Tamaki et al. [10] described how the KEEP schemes reduce the entropy conservation errors and thus improve numerical robustness. This entropy analysis also leads to the redefinition of the KEEP schemes and the KEEP schemes with more reduced entropy conservation errors. Furthermore, while the KEP and KEEP schemes and entropy conservative schemes [17, 18, 19, 20, 21] have generally been developed individually, Tamaki et al. [10] bridged those schemes with respect to the entropy conservation errors.

3.3 Spectral characteristics of split convective forms in finite difference methods

The convective terms are discretized in split forms in the KEP and KEEP schemes. For example, the convective terms of the KEEP scheme shown in Eq. (9) are discretized in the cubic split form:

$$\widetilde{\Phi}_j|_{(m\pm\frac{1}{2})} \equiv \frac{\rho|_{(m)}+\rho|_{(m\pm1)}}{2}\frac{\phi|_{(m)}+\phi|_{(m\pm1)}}{2}\frac{u_j|_{(m)}+u_j|_{(m\pm1)}}{2}, \tag{21}$$

where ϕ is a general transport scalar and corresponds to 1, u_i, and e in the mass, momentum, and internal energy equations. This cubic split form corresponds to discretizing the convective term $\frac{\partial \rho\phi u_j}{\partial x_j}$ as the sum of the conservative and non-conservative terms as:

$$\frac{\partial \rho\phi u}{\partial x} \approx \frac{1}{4}\left(\frac{\delta\rho\phi u}{\delta x}+u\frac{\delta\rho\phi}{\delta x}+\rho\frac{\delta\phi u}{\delta x}+\phi\frac{\delta\rho u}{\delta x}+\rho\phi\frac{\delta u}{\delta x}+\phi u\frac{\delta\rho}{\delta x}+\rho u\frac{\delta\phi}{\delta x}\right), \tag{22}$$

where δ denotes spatial discretization. Other split forms may be found in Refs. [22, 23, 24, 25].

In addition to the studies of the KEP and KEEP schemes based on the split convective forms, the prior studies [23, 24] examined the spectral property of the split forms and showed that the split convective forms are capable of reducing aliasing errors in spectral methods. Based on the discussions in Refs. [23, 24], it has been discussed that the split convective forms are capable of reducing aliasing errors, contributing to numerical stability enhancement, even in finite difference methods. However, Ref. [11] very recently revealed that the split convective forms do not reduce aliasing errors but rather may increase them in the finite difference framework. This finding is completely opposite to what has been discussed in the community. Also, this finding suggests that the enhanced preservation property of the secondary conservative variables, such as the kinetic energy and entropy, may have a more dominant impact on the enhanced numerical robustness of the KEP and KEEP schemes in finite difference methods because, theoretically, aliasing errors are not reduced by the split convective forms in finite difference methods. Furthermore, Ref. [11] derived the modified wavenumber of the split forms and showed that the modified wavenumber of the split forms is larger than that of the convectional divergence form.

3.4 A spatially and temporally conservative KEEP scheme

Subbareddy and Candler [3] and Morinishi [25] proposed the numerical schemes that preserve the kinetic energy in both space and time, while most of the previous studies on the KEP schemes have considered only spatial kinetic energy preservation. Regarding the KEEP schemes, Asada et al. [12] recently proposed a fully (i.e., spatially and temporally) conservative KEEP scheme. The proposed scheme has been developed introducing the auxiliary velocity, density, and internal energy for the temporal discretization and has

demonstrated stable and non-dissipative compressible flow computations with large computational time-step size in an inviscid numerical test.

3.5 A KEEP scheme for unstructured finite volume methods

Kuya et al. [13] recently proposed a KEEP scheme for unstructured finite volume methods. In the proposed KEEP finite volume scheme, cell-vertex discretization is employed in order to achieve second-order accuracy in space on simplex grids and arbitrary grids with satisfying the aforementioned analytical relations. In numerical tests, the KEEP finite volume scheme also successfully performs long-time stable computations without using numerical dissipation on various unstructured grids.

In Asada and Kawai [15] and Tamaki et al. [16], a block-structured Cartesian solver is used to perform high-Reynolds number LES of whole aircraft configurations using the LES wall model [14] and the KEEP schemes [6, 7]. However, finite volume solvers are still widely used to conduct flow numerical simulations around complex geometries. Therefore, extending the KEEP schemes to unstructured finite volume methods will provide more options for performing high-fidelity flow computations around complex geometries.

4 Numerical tests: inviscid Taylor-Green vortex at M_0=0.4

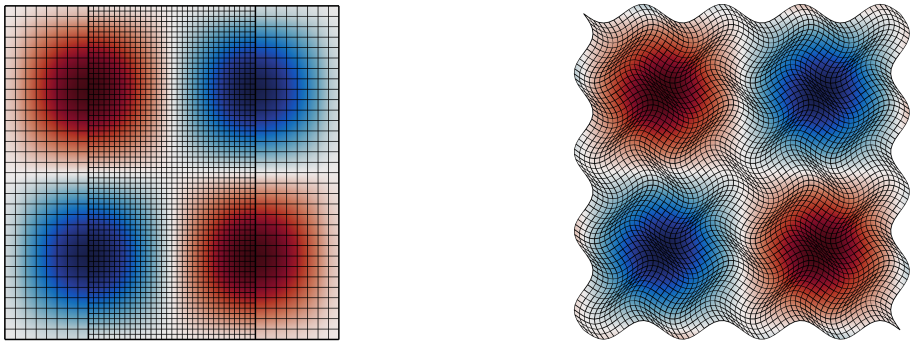

(a) Cartesian grid with non-conforming boundaries (b) Distorted curvilinear grid

Figure 2: Computational grids used in inviscid Taylor-Green vortex test. The colors denote the initial z-vorticity.

The capability of the KEEP schemes proposed in Refs. [6, 7, 8] is examined by inviscid Taylor-Green vortex (TGV) computations on two different computational grids shown in Fig. 2: Cartesian grid where two non-conforming grid boundaries are contained (Fig. 2(a)), and largely distorted curvilinear grid (Fig. 2(b)). Each grid size of the coarse and fine grids of the Cartesian grid corresponds to those of 32^3 and 64^3 periodic boxes, respectively. The distorted curvilinear grid also consists of 64^3 grid points. Those computational grids are the same as those used in Refs. [7] and [8], respectively, and further details about the computational grids used here can be found in those references. For reference, a 64^3 Cartesian grid with uniformly distributed grid points is also used.

The initial flow conditions are set by

$$
\begin{aligned}
&\rho = \rho_0, \\
&u = M_0 \sin(x)\cos(y)\cos(z), \\
&v = -M_0 \cos(x)\sin(y)\cos(z), \\
&w = 0, \\
&p = \frac{1}{\gamma} + \frac{\rho_0 M_0^2}{16}\left[\cos(2x)+\cos(2y)\right]\left[\cos(2z)+2\right].
\end{aligned}
$$

The initial density ρ_0 and Mach number M_0 are set to 1.0 and 0.4, respectively. Time advancement is

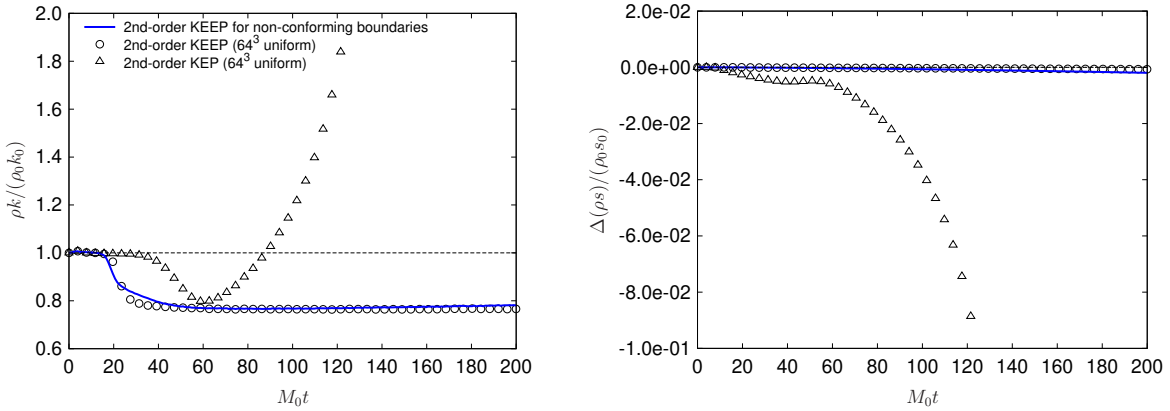

(a) Total kinetic energy (b) Total entropy

Figure 3: Time evolution of total kinetic energy and total entropy on Cartesian grid with non-conforming boundaries.

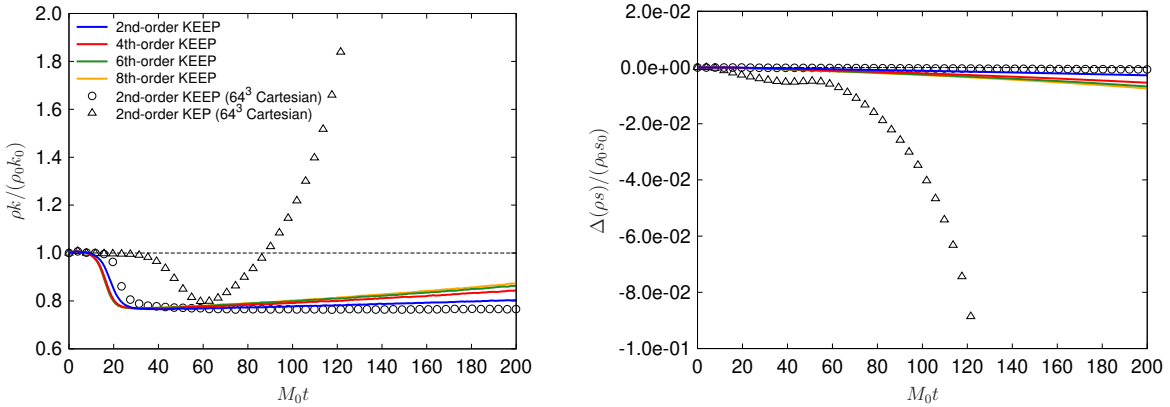

(a) Total kinetic energy (b) Total entropy

Figure 4: Time evolution of total kinetic energy and total entropy on distorted curvilinear grid.

performed using the four-stage fourth-order Runge-Kutta scheme [26]. A CFL number is set to about 0.1. Refs. [6, 8] confirmed that the CFL number of 0.1 is sufficiently small to avoid time integration errors. The KEP schemes [1, 4] are also employed for comparison, in addition to the KEEP schemes.

Figure 3 shows the time evolution of the total kinetic energy and total entropy ($\Delta\rho s$=$\rho_0 s_0$-ρs) on the Cartesian grid with non-conforming grid boundaries. The total kinetic energy and total entropy are obtained by integrating those values over the whole computational domain. The inviscid TGV problem is well known as a test case that is difficult to perform stably without the use of numerical dissipation. The difficulty of this problem can be confirmed from the computation of the KEP scheme on the 64^3 Cartesian grid that numerically diverges around M_0t=120. On the other hand, the KEEP schemes described in sections 2.2 and 2.3 stably conduct a long-time inviscid computation even on the Cartesian grid with non-conforming boundaries. When the KEEP schemes are used, both the kinetic energy and entropy are preserved well. In contrast, the KEP scheme on the 64^3 Cartesian grid increases the total kinetic energy and reduces the total entropy nonphysically. The kinetic energy reduction seen around M_0t=20 in the KEEP scheme computations is due to the compressible effect [6].

Figure 4 shows the time evolution of the total kinetic energy and total entropy on the distorted curvilinear grid. The second- to eight-order accurate KEEP schemes described in section 2.4 achieve long-time inviscid computations stably even on the largely distorted curvilinear grid. Although the total kinetic energy gradually increases, and the total entropy gradually decreases due to the long-time integration in the KEEP

scheme computations, the computations are still stably conducted at least until M_0t=200. By comparing with the results of the KEP scheme on the Cartesian grid, it can be confirmed how stable the high-order accurate KEEP schemes proposed in Ref. [8] are.

5 Conclusions

The present study has comprehensively discussed the kinetic energy and entropy preserving (KEEP) schemes, which were developed to realize high Reynolds number large-eddy simulation (LES) around complex geometries. Among the recent research progress made by our research group on the KEEP schemes, here we focus on 1) second-order accurate KEEP scheme in Cartesian coordinates [6] (section 2.2), 2) KEEP scheme for non-conforming block boundaries on block-structured Cartesian grids [7] (section 2.3), and 3) high-order accurate KEEP scheme in generalized curvilinear coordinates [8] (section 2.4). The derivation background of the KEEP schemes is also described in section 2.1. In addition, we discuss other research subjects related to the KEEP schemes in Section 3: 4) split convective form maintaining velocity and pressure equilibrium at contact discontinuity [9], 5) entropy conservation error analysis of KEEP schemes [10], 6) spectral characteristics of split convective forms in finite difference methods [11], 7) spatially and temporally conservative KEEP scheme [12], and 8) KEEP scheme for unstructured finite volume methods [13]. Wall-modeled LES of whole aircraft configurations were recently realized using the KEEP schemes described in sections 2.2 and 2.3, and it has been demonstrated how useful the KEEP schemes are for conducting high-fidelity computations around complex geometries stably.

References

[1] Antony Jameson. Formulation of kinetic energy preserving conservative schemes for gas dynamics and direct numerical simulation of one-dimensional viscous compressible flow in a shock tube using entropy and kinetic energy preserving schemes. *Journal of Scientific Computing*, 34(2):188–208, 2008.

[2] J. C. Kok. A high-order low-dispersion symmetry-preserving finite-volume method for compressible flow on curvilinear grids. *Journal of Computational Physics*, 228(18):6811–6832, 2009.

[3] Pramod K Subbareddy and Graham V Candler. A fully discrete, kinetic energy consistent finite-volume scheme for compressible flows. *Journal of Computational Physics*, 228(5):1347–1364, 2009.

[4] Sergio Pirozzoli. Generalized conservative approximations of split convective derivative operators. *Journal of Computational Physics*, 229(19):7180–7190, 2010.

[5] Sergio Pirozzoli. Stabilized non-dissipative approximations of Euler equations in generalized curvilinear coordinates. *Journal of Computational Physics*, 230(8):2997–3014, 2011.

[6] Yuichi Kuya, Kosuke Totani, and Soshi Kawai. Kinetic energy and entropy preserving schemes for compressible flows by split convective forms. *Journal of Computational Physics*, 375:823–853, 2018.

[7] Yuichi Kuya and Soshi Kawai. A stable and non-dissipative kinetic energy and entropy preserving (KEEP) scheme for non-conforming block boundaries on cartesian grids. *Computers & Fluids*, page 104427, 2020.

[8] Yuichi Kuya and Soshi Kawai. High-order accurate kinetic-energy and entropy preserving (KEEP) schemes on curvilinear grids. *Journal of Computational Physics*, 442:110482, 2021.

[9] Nao Shima, Yuichi Kuya, Yoshiharu Tamaki, and Soshi Kawai. Preventing spurious pressure oscillations in split convective form discretization for compressible flows. *Journal of Computational Physics*, 427:110060, 2021.

[10] Yoshiharu Tamaki, Yuichi Kuya, and Soshi Kawai. Comprehensive analysis of entropy conservation property of non-dissipative schemes for compressible flows: KEEP scheme redefined. (in revision).

[11] Yuichi Kuya and Soshi Kawai. Modified wavenumber and aliasing errors of split convective forms for compressible flows. *Journal of Computational Physics*, 464:111336, 2022.

[12] Hiroyuki Asada, Kanako Maruyama, and Soshi Kawai. Fully conservative kinetic-energy and entropy preserving (KEEP) scheme for compressible flows. (under review).

[13] Yuichi Kuya, Wataru Okumura, and Keisuke Sawada. A kinetic energy and entropy preserving (KEEP) finite volume scheme on unstructured grids for compressible flows. (under review).

[14] Yoshiharu Tamaki and Soshi Kawai. Wall modeling for large-eddy simulation on non-body-conforming cartesian grids. *Phys. Rev. Fluids*, 6:114603, Nov 2021.

[15] Hiroyuki Asada and Soshi Kawai. LES of full aircraft configuration using non-dissipative KEEP scheme with conservative explicit filter. In *AIAA SCITECH 2022 Forum*, 2022. AIAA Paper 2022-0449.

[16] Yoshiharu Tamaki, Hiroyuki Asada, Ryo Takaki, and Soshi Kawai. Wall-modeled LES around the CRM-HL using fully-automated Cartesian-grid-based flow solver FFVHC-ACE. In *AIAA AVIATION 2022 Forum*, 2022.

[17] Eitan Tadmor. The numerical viscosity of entropy stable schemes for systems of conservation laws. I. *Mathematics of Computation*, 49(179):91–103, 1987.

[18] Eitan Tadmor. Entropy stability theory for difference approximations of nonlinear conservation laws and related time-dependent problems. *Acta Numerica*, 12:451–512, 2003.

[19] Farzad Ismail and Philip L Roe. Affordable, entropy-consistent euler flux functions ii: Entropy production at shocks. *Journal of Computational Physics*, 228(15):5410–5436, 2009.

[20] Praveen Chandrashekar. Kinetic energy preserving and entropy stable finite volume schemes for compressible euler and navier-stokes equations. *Communications in Computational Physics*, 14(5):1252–1286, 2013.

[21] Hendrik Ranocha. *Generalised summation-by-parts operators and entropy stability of numerical methods for hyperbolic balance laws*. PhD thesis, TU Braunschweig, 2018.

[22] William John Feiereisen. *Numerical simulation of a compressible, homogeneous turbulent shear flow*. PhD thesis, Stanford University, 1981.

[23] G. A. Blaisdell, E. T. Spyropoulos, and J. H. Qin. The effect of the formulation of nonlinear terms on aliasing errors in spectral methods. *Applied Numerical Mathematics*, 21(3):207–219, 1996.

[24] Christopher A Kennedy and Andrea Gruber. Reduced aliasing formulations of the convective terms within the Navier–Stokes equations for a compressible fluid. *Journal of Computational Physics*, 227(3):1676–1700, 2008.

[25] Yohei Morinishi. Skew-symmetric form of convective terms and fully conservative finite difference schemes for variable density low-Mach number flows. *Journal of Computational Physics*, 229(2):276–300, 2010.

[26] Wilhelm Kutta. *Beitrag zur näherungsweisen integration totaler differentialgleichungen*. PhD thesis, Ludwig-Maximilians-Universität München, 1901.